ChemComm

COMMUNICATION

View Article Online
View Journal | View Issue

Rapid construction of an effective antifouling layer on a Au surface *via* electrodeposition†

Cite this: *Chem. Commun.*, 2014, 50, 6793

Received 20th February 2014,
Accepted 6th May 2014

DOI: 10.1039/c4cc01329h

www.rsc.org/chemcomm

Bor-Ran Li,‡[a] Mo-Yuan Shen,‡[a] Hsiao-hua Yu[b] and Yaw-Kuen Li*[a]

A new approach to immobilize zwitterionic molecules rapidly and highly efficiently on a gold surface applies aniline-based electrodeposition. The zwitterion-functionalized antifouling surface enables a decrease of the adsorption of non-specific proteins by 95% from fetal bovine serum (FBS, 10%).

Biosensors have drawn much attention because of their potential to greatly improve biomedical research,[1–4] drug discovery,[5,6] environmental monitoring,[7] and diagnosis of many diseases.[8–10] In particular, a biosensor applied to the clinical diagnosis of epidemic diseases,[11] long-term nursing of chronic diseases,[12] and early diagnosis of cancers[13] could save many lives around the world. To improve various properties of biosensors with the latest technology is hence of continual interest to engineers and scientists. The quartz crystal microbalance (QCM),[14] an ultra-sensitive balance capable of measuring changes in mass at the molecular level, is one of the most attractive biosensors that has been commercialized. The structure of a QCM chip is robust; the measurement is processed in real time, free of labels, and almost independent of the ionic strength. A QCM is thus supposed to be an ideal system for biological sensing, and has been established to detect various biomolecules *via* the specific recognition of target analytes with the corresponding receptors (*i.e.* antibodies) immobilized on the Au surface of the device.[15] The nonspecific binding between the proteins in a patient's serum and the Au surface of a QCM is a critical problem that might greatly decrease the sensitivity and reliability of the detection. To decrease the nonspecific interaction between the components of plasma and the Au surface is thus an important issue for sensitive and specific sensing of biological matrices.

Goda *et al.*[16] demonstrated that thiol-functionalized zwitterions were chemisorbed to form a self-assembled monolayer (SAM) on the Au surface of a QCM chip *via* a Au–S bond. *Via* ionic solvation, the zwitterionic layer can strongly trap water molecules on the surface of the chip. The expulsion of water molecules from between the protein and the zwitterion surface becomes difficult leading to the reduction of non-specific protein adsorption on the chip. The presence of the inert zwitterionic layer decreased the non-specific binding up to 60–70% from the dilute serum (10% fetal bovine serum, FBS), indicating that modifying a QCM surface with zwitterions is an ideal strategy to create antifouling platforms for sensitive and specific detection involving a clinical sample.[17,18] Although a thiol-SAM is readily prepared on the Au surface of a QCM chip on immersing the substrate in a dilute solution of zwitterionic thiols, the thiol-SAM process requires 12 to 72 h at room temperature.[19,20] A Au surface of high quality and pure reagents are essential to avoid defects in the monolayer formation.[21] Unlike the smooth Au surface on SPR, a bumpy sub-micrometre structure of a Au surface on a QCM chip is commonly observed because of its advantage of enlarging the binding area to enhance sensitivity.[22] Defects (*e.g.* monatomic vacancy islands) on the rough Au surface are easily formed upon modification of a zwitterionic layer using thiol-SAM approaches. Intermolecular electrostatic repulsion between zwitterionic molecules might also cause the formation of a non-uniform SAM layer that consequently produces a poor zwitterion density and results in a limited antifouling effect. The development of a new approach to decrease the duration of reaction and to achieve a uniform antifouling layer on the Au surface is hence highly desirable.

Here, we demonstrate a new approach to directly modify the zwitterionic molecule, dimethyl-ammonio propane-1-sulfonate (sulfobetaine or SB),[23,24] on the Au surface of the QCM chip *via* electrodeposition. In the first step, sulfobetaine (SB) is conjugated with an aniline functional group to from 3-[(4-aminophenyl)-dimethylammonio]propane-1-sulfonate (referred to as aminophenyl sulfobetaine or AP-SB in this report). Upon optimizing the conditions, AP-SB can be efficaciously synthesized in a yield >70%.

[a] *Department of Applied Chemistry, National Chiao Tung University, Hsinchu, Taiwan. E-mail: ykl@cc.nctu.edu.tw*
[b] *Institute of Chemistry, Academia Sinica, Taipei, Taiwan*

† Electronic supplementary information (ESI) available: Fig. S1–S6 and Section S1–S7. See DOI: 10.1039/c4cc01329h

‡ Bor-Ran Li and Mo-Yuan Shen made equal contributions to this work.

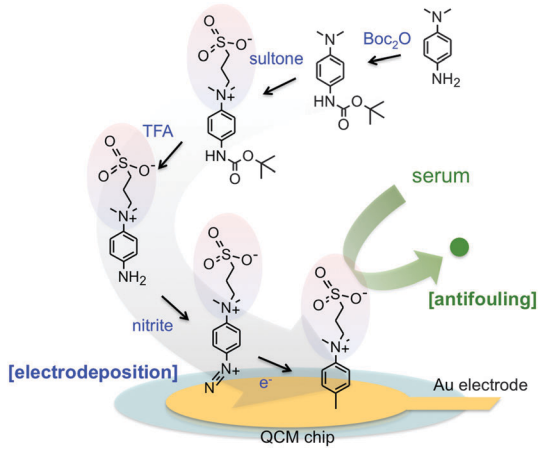

Scheme 1 Schematic illustration of the synthesis and deposition of anti-fouling zwitterions on the gold electrode.

Unlike thiol-sulfobetaine, (HS-SB) can automatically chemisorb to form a SAM on the QCM chip through chemical binding between the mercapto group and Au; the AP-SB modification operates through the *in situ* generation of the aminophenyl diazonium cation in aqueous HCl (0.5 M) and $NaNO_2$ at an equivalent concentration, and subsequently coating onto the Au surface by electrochemical reduction *via* cyclic voltammetry (Scheme 1),[25,26] which can be completed in a few minutes. The details of thiol self-assembly, electrodeposition, and organic synthesis are provided in Fig. S1 and S2, and Section S2, S3, S7 and S8 of the ESI.† The surface modification is confirmed by ESCA (Fig. S3, ESI†).

Cyclic voltammetry is utilized to evaluate the efficiency of thiol-SAM and the aniline electroplating modification. As the results in Fig. 1A and B show, the bare gold electrode (black line) reveals higher oxidation and reduction current peaks (I_p) in a solution of 10 mM $[Fe(CN)_6]^{3-}$ as the indicator dissolved in PBS (phosphate buffered saline, containing 137 mM NaCl, 2.7 mM KCl, 10 mM Na_2HPO_4 and 2 mM KH_2PO_4, pH 7.2) at a scan rate of 100 mV s^{-1}. When the Au electrodes were coated with an octyl moiety (as insulated layer) by either thiol-SAM (Fig. 1A) or aniline-based electrodeposition (Fig. 1B) for varied durations, the exposed areas of Au electrodes were decreased, consequently resulting in smaller redox peaks. Whereas the electrode modified with aniline-based electrodeposition for 1 to 3 min greatly decreased the I_p peaks (blue and cyan lines in Fig. 1B), the electrode modified with a thiol-SAM approach for 1 h, 3 h or even 3 days induced only smaller effects on the I_p peak changes (red, orange and violet lines in Fig. 1A). Similar results were obtained when RuHex, $[Ru(NH_3)_6]^{3+}$, was used as the redox indicator (Fig. S4, ESI†).

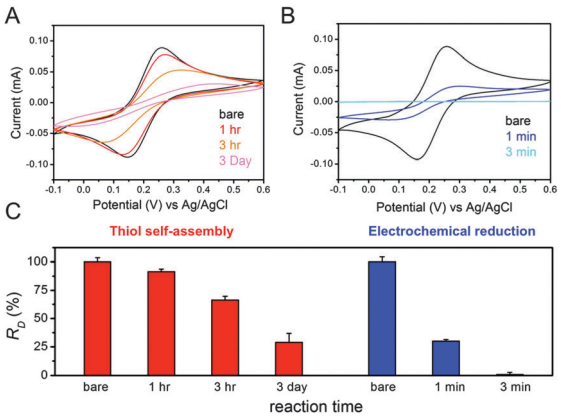

Fig. 1 (A) Cyclic voltammogram of Au electrodes bare (black) and modified with 1-octanethiol for 1 h (red), 3 h (orange), and 3 days (violet) in a solution of ferricyanide (10 mM, dissolved in 1 × PBS) at a scan rate of 100 mV s^{-1}. (B) CV curves measured with Au electrodes bare (black) and electrodeposited with 4-octylaniline in 1 (blue) and 3 min (cyan). (C) The histogram shows a comparison of the relative density of surface modification (R_D) of Au electrodes modified with 1-octanethiol (red) for 0 h, 1 h, 3 h and 3 days and 4-octylaniline (blue) for 0 min, 1 min, and 3 min. The error bars represent the standard deviations of three measurements.

A relationship between the electrode area and I_p (A_e) is described using the Randles–Sevcik eqn (1):

$$I_p = 0.4463\, nFA_eC\sqrt{\frac{nFvD}{RT}} \propto A_e \qquad (1)$$

in which I_p = measured peak current/A; n = number of electrons transferred in the redox event, F = faraday constant/C mol^{-1}, A_e = exposed area of the Au electrode/cm^2, C = concentration of ferricyanide/mol cm^{-3}, ν = scan rate/V s^{-1}, D = diffusion coefficient/cm^2 s^{-1}, R = gas constant, and T = temperature/deg F. In addition, the relative density of surface modification (R_D) is defined as $A_{e.mod}/A_{e.t}$ (eqn (2)). Therefore,

$$R_D = \frac{A_{e.mod}}{A_{e.t}} = \frac{A_{e.t} - A_{e.unmod}}{A_{e.t}} = \frac{I_{p.max} - I_p}{I_{p.max}} = \frac{\Delta I_p}{I_{p.max}} \qquad (2)$$

where $A_{e.mod}$ is the area of the Au electrode modified, and $A_{e.t}$ is the total surface area of the Au electrode. $I_{p.max}$ is the I_p of the current peak of CV scanning by a bare Au electrode. R_D is utilized to quantify the immobilization. Fig. 1C shows the R_D of the electrodes modified with 1-octanethiol and 4-octylaniline for varied durations. The histogram reveals that 99 ± 1% surface area of the Au electrode is efficiently modified by the aniline-based electrodeposition in 3 min, but the electrode modified with thiol-SAM for 3 days still leaves 30 ± 5% unmodified area. These results indicate that aniline-based electrodeposition is a rapid and highly efficient method for chemical modification of a bumpy Au surface.

As shown in the illustrations in the upper panel of Fig. 2A, a higher SB density on the QCM chip might result in effective antifouling ability. To confirm the antifouling properties of a Au surface modified with SB by thiol-SAM and aniline-based electrodeposition, we employed the QCM chips modified by these two methods to compare the non-specific adsorption of dilute serum in real-time monitoring. Whereas fetal bovine serum (10% FBS, in PBS, pH 7.2) caused a prominent decrease of the resonance frequency (130 ± 10 Hz) on the bare QCM chip, the same sample induced a smaller frequency change (45 ± 10 Hz) on the HS-SB modified chip and a minor frequency change (6 ± 3 Hz) on the AP-SB electrodeposited QCM chip. The frequency change can serve to estimate the accumulated change in mass based on the Sauerbrey eqn (3),[27] in which f_0 = resonant frequency/Hz, Δf = frequency change/Hz, Δm = mass

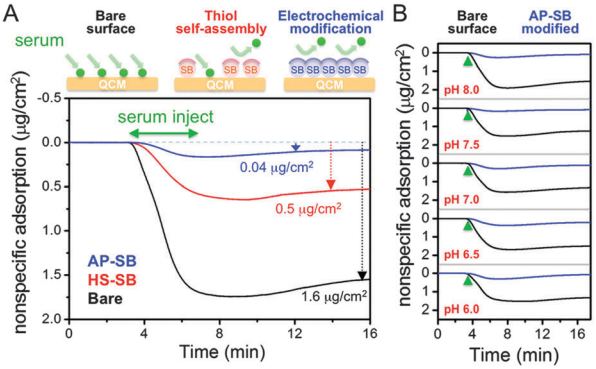

Fig. 2 (A) Real-time recording of the Δ frequency responses to FBS (10%) with AP-SB-electrodeposited (blue), HS-SB SAM-coated (red), and unmodified (black) QCM devices in PBS buffer (pH 7.2). (B) Comparison of responses of bare (black) and electroplated SB QCM devices to FBS (10%) at pH 6.0, 6.5, 7.0, 7.5 and 8.0. Green arrows indicate the point of FBS injection.

change/g, A = area of electrodes/cm^2, ρ_q = density of quartz and μ_q = shear modulus of quartz.

$$\Delta f = -\frac{2{f_0}^2}{A\sqrt{\rho_q \mu_q}}\Delta m \qquad (3)$$

As the results in Fig. 2A show, QCM with the zwitterionic layer immobilized by electrodeposition is demonstrated to adsorp non-specific bound proteins (0.04 μg cm^{-2}) (blue line) to a lesser extent than a bare (1.6 μg cm^{-2}) (black line) surface or the one modified by the thiol-SAM approach (0.6 μg cm^{-2}) (red line). As the pK_a of sulfonic acid is relatively low, the SB is expected to maintain a zwitterionic form in a wide range of pH. For this reason, a SB-modified QCM chip exhibits pH-independent antifouling ability, particularly in the pH range 6–8, the common conditions of bio-analysis or diagnosis (Fig. 2B). Since low ionic strength (<100 mM) may increase non-specific protein adsorption,[28,29] a high buffer concentration (150 mM) is employed in this study. The stability of the SB-modified chip is monitored for more than 2 weeks with no significant loss of the antifouling ability (Fig. S5, ESI†).

We utilized fluorescence images to display the antifouling ability of Au electrodes with and without the SB modification. We dropped a red fluorescent protein (mCherry) onto the silicon substrate with the micro-patterned Au electrodes. As the control experiment shows (Fig. 3A), a bare substrate without mCherry treatment revealed no fluorescence emission. After incubation for 1 h with the concentrated mCherry protein (10 mg mL^{-1}, approximately equivalent to the concentration of total proteins in 10% serum), non-specific binding, resulting in red fluorescence, is clearly revealed on the bare Au electrodes (Fig. 3B), but almost no mCherry protein adhered to the electrode selectively coated with SB by electrodeposition (Fig. 3C). The relative fluorescence intensities in Fig. 3A(i), B(i), and C(i) quantified by the Photoshop program, is 0, 116, and 4, respectively. The bottom panels (Fig. 3A(ii), B(ii), and C(ii)) show bright-field images at the same positions. The red colour (not fluorescence)

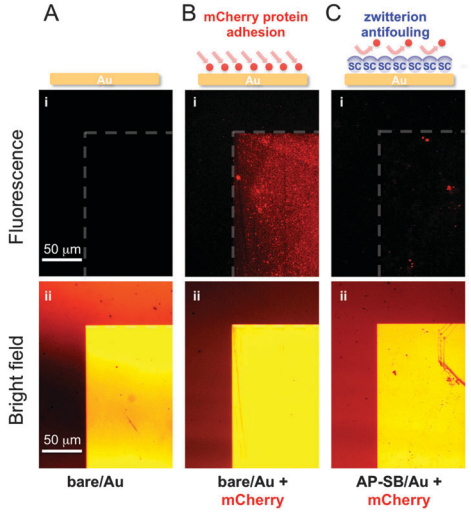

Fig. 3 Images of adhesion of the mCherry fluorescent protein on a micro-patterned gold electrode on a photoresist-(LOR-5B)-preserved silicon substrate. (A) Fluorescent (i) and bright-field (ii) images of a bare Au electrode without mCherry treatment. (B) Images of a bare Au electrode incubated with the mCherry fluorescent protein (10 mg mL^{-1}) for 1 h. (C) Images of the AP-SB-modified Au electrode incubated with the mCherry fluorescent protein (10 mg mL^{-1}) for 1 h.

shown in these bright-field images resulted from the reflection of incident light.

In summary, we present a synthesis of an aniline-based zwitterionic molecule (AP-SB) in a high yield (>70%) that is demonstrated to be a key reagent to improve the surface modification of Au chips by electrodeposition. Relative to a conventional thiol-SAM approach, electrodeposition has the advantages of decreasing the duration of reaction from hours or even days to 3 min and increasing the SB modification density, resulting in significantly decreased non-specific binding up to 95 ± 3% from the dilute FBS. The SB-modified chip clearly demonstrated much better antifouling properties than those of bare gold and the hydrophobic surface (Fig. S6, ESI†). The platform demonstrated herein is highly useful to improve the sensitivity and reliability of a biosensor using Au as the sensory chip. It is also useful for carbon,[30] ITO,[31] and other electrodes.[32]

The Ministry of Science and Technology of Taiwan (NSC 101-2120-M-009-011-CC1) and the Center for Interdisciplinary Science (CIS) of National Chiao Tung University of Taiwan under MOE 5Y50B project financially supported this research.

Notes and references

1 J. Wang, *Chem. Rev.*, 2008, **108**, 814–825.
2 J. T. Sheu, C. C. Chen, K. S. Chang and Y. K. Li, *Biosens. Bioelectron.*, 2008, **23**, 1883–1886.
3 Y. Liu, X. Dong and P. Chen, *Chem. Rev.*, 2012, **41**, 2283–2307.
4 B. R. Li, C. C. Chen, R. U. Kumar and Y. T. Chen, *Analyst*, 2014, **139**, 1589–1608.
5 M. A. Cooper, *Nat. Rev. Drug Discovery*, 2002, **1**, 515–528.
6 M. F. Templin, D. Stoll, M. Schrenk, P. C. Traub, C. F. Vohringer and T. O. Joos, *Drug Discovery Today*, 2002, **7**, 815–822.
7 F. Long, A. Zhu and H. Shi, *Sensors*, 2013, **13**, 13928–13948.
8 K. I. Chen, B. R. Li and Y. T. Chen, *Nano Today*, 2011, **6**, 131–154.

9 B. R. Li, C. W. Chen, W. L. Yang, T. Y. Lin, C. Y. Pan and Y. T. Chen, *Biosens. Bioelectron.*, 2013, **45**, 252–259.
10 B. R. Li, Y. J. Hsieh, Y. X. Chen, Y. T. Chung, C. Y. Pan and Y. T. Chen, *J. Am. Chem. Soc.*, 2013, **135**, 16034–16037.
11 R. B. Belshe, *N. Engl. J. Med.*, 2005, **353**, 2209–2211.
12 H. M. So, K. Won, Y. H. Kim, B. K. Kim, B. H. Ryu, P. S. Na, H. Kim and J. O. Lee, *J. Am. Chem. Soc.*, 2005, **127**, 11906–11907.
13 M. J. Barry, *N. Engl. J. Med.*, 2001, **344**, 1373–1377.
14 W. H. King, *Anal. Chem.*, 1964, **36**, 1735–1739.
15 C. I. Cheng, Y. P. Chang and Y. H. Chu, *Chem. Soc. Rev.*, 2012, **41**, 1947–1971.
16 T. Goda, M. Tabata, M. Sanjoh, M. Uchimura, Y. Iwasaki and Y. Miyahara, *Chem. Commun.*, 2013, **49**, 8683–8685.
17 H. Zhao, B. Zhu, S. C. Luo, H. A. Lin, A. Nakao, Y. Yamashita and H. H. Yu, *ACS Appl. Mater. Interfaces*, 2013, **5**, 4536–4543.
18 L. Zhang, Z. Cao, T. Bai, L. Carr, J. R. Ella-Menye, C. Irvin, B. D. Ratner and S. Jiang, *Nat. Biotechnol.*, 2013, **31**, 553–556.
19 J. C. Love, L. A. Estroff, J. K. Kriebel, R. G. Nuzzo and G. M. Whitesides, *Chem. Rev.*, 2005, **105**, 1103–1169.
20 H. B. Akkerman, P. W. Blom, D. M. de Leeuw and B. de Boer, *Nature*, 2006, **441**, 69–72.
21 P. Fenter, A. Eberhardt and P. Eisenberger, *Science*, 1994, **266**, 1216–1218.
22 N. L. Rosi and C. A. Mirkin, *Chem. Rev.*, 2005, **105**, 1547–1562.
23 Z. Zhang, J. Borenstein, L. Guiney, R. Miller, S. Sukavaneshvar and C. Loose, *Lab Chip*, 2013, **13**, 1963–1968.
24 G. Li, G. Cheng, H. Xue, S. Chen, F. Zhang and S. Jiang, *Biomaterials*, 2008, **29**, 4592–4597.
25 J. Lyskawa and D. Bélanger, *Chem. Mater.*, 2006, **18**, 4755–4763.
26 I. Jabin, C. Mangeney, C. Roux, O. Reinaud, L. Santos, J. F. Bergamini, P. Hapiot and C. Lagrost, *Nat. Commun.*, 2012, **3**, 1130.
27 G. Sauerbrey, *Phys. Z.*, 1959, **155**, 206–222.
28 R. E. Holmlin, X. Chen, R. G. Chapman, S. Takayama and G. M. Whitesides, *Langmuir*, 2001, **17**, 2841–2850.
29 E. Ostuni, R. G. Chapman, M. N. Liang, G. Meluleni, G. Pier, D. E. Ingber and G. M. Whitesides, *Langmuir*, 2001, **17**, 6336–6343.
30 C. Dalmolin, S. C. Canobre, S. R. Biaggio, R. C. Rocha-Filho and N. Bocchi, *Electrochem. Commun.*, 2005, **578**, 9–15.
31 E. Venancio, C. Costa, S. Machado and A. Motheo, *Electrochem. Commun.*, 2001, **3**, 229–233.
32 J. Pinson and F. Podvorica, *Chem. Soc. Rev.*, 2005, **34**, 429–439.

